Additive manufacturing in radiation oncology: a review of clinical practice, emerging trends and research opportunities

OPEN ACCESS
IOP Publishing | IMMT
International Journal of Extreme Manufacturing
Int. J. Extrem. Manuf. 2 (2020) 012003 (20pp)
https://doi.org/10.1088/2631-7990/ab70af

Topical Review

Additive manufacturing in radiation oncology: a review of clinical practice, emerging trends and research opportunities

Rance Tino[1,2,3], Martin Leary[1,3], Adam Yeo[2], Elizabeth Kyriakou[1,2], Tomas Kron[2,3,4] and Milan Brandt[1,3]

[1] RMIT Centre for Additive Manufacture, School of Engineering, RMIT University, Melbourne, Australia
[2] Physical Sciences Department, Peter MacCallum Cancer Centre, Melbourne, Australia
[3] ARC Industrial Transformation Training Centre in Additive Biomanufacturing, Queensland University of Technology, Brisbane, Australia
[4] Centre for Medical Radiation Physics, University of Wollongong, Wollongong Australia

E-mail: milan.brandt@rmit.edu.au

Received 15 December 2019, revised 15 January 2020
Accepted for publication 26 January 2020
Published 17 February 2020

Abstract

The additive manufacturing (AM) process plays an important role in enabling cross-disciplinary research in engineering and personalised medicine. Commercially available clinical tools currently utilised in radiotherapy are typically based on traditional manufacturing processes, often leading to non-conformal geometries, time-consuming manufacturing process and high costs. An emerging application explores the design and development of patient-specific clinical tools using AM to optimise treatment outcomes among cancer patients receiving radiation therapy. In this review, we:

- highlight the key advantages of AM in radiotherapy where rapid prototyping allows for patient-specific manufacture
- explore common clinical workflows involving radiotherapy tools such as bolus, compensators, anthropomorphic phantoms, immobilisers, and brachytherapy moulds; and
- investigate how current AM processes are exploited by researchers to achieve patient tissue-like imaging and dose attenuations.

Finally, significant AM research opportunities in this space are highlighted for their future advancements in radiotherapy for diagnostic and clinical research applications.

Keywords: additive manufacturing, radiotherapy tools, dosimetry, EBRT, patient-specific, cancer treatment, quality assurance

(Some figures may appear in colour only in the online journal)

1. Introduction

The additive manufacturing (AM) process has produced countless research advancements not only in the engineering research and development space but also in medical applications. Well known applications for AM in the medical

space involves the fabrication of patient-specific surgical models [1], bone implants [2–6], dental moulds and implants [7–10], scaffolds for tissue engineering applications [11–17], and the fabrication of inexpensive and personalised radiotherapy tools utilised by clinicians in radiation therapy (RT) to improve patient treatment outcomes. During RT, it is common to use beam modifiers during radiotherapy to accommodate irregular patient surfaces, for instance, wedge filters [18], which are used to modify the isodose distribution to a certain amount to achieve dose homogeneity, as well as electron beam cut-outs [19], which are utilised to shape beams according to a specified cut-out geometry. Other forms of beam modifiers include boluses [20] and compensators [21], which are personalised devices and can achieve better isodose distributions for more irregular surfaces. Another commonly used clinical tool are immobilisers [22], which are used by radiotherapists as fixation devices for patients during treatment to minimise body movements and avoid the irradiation of healthy tissues. More complex radiotherapy clinical tools include brachytherapy moulds for localised cancer treatment using radioactive seeds, in particular for prostate cancer procedures [23] and the use of in-vitro dosimetry models such as anthropomorphic radiotherapy phantoms to validate the overall deliverability of treatment plans involving imaging and dosimetry [24, 25].

Without proper clinical interventions by medical physicists, radiotherapists and oncologists, these clinical devices fall short as they do not exactly replicate patients in terms of body dimensions and tissue inhomogeneities. For instance, commercially available radiotherapy phantoms to validate patient treatment plans were observed to produce a lack of dose information due to the unaccounted presence of patient-specific lesions. Furthermore, these phantoms are fabricated through moulding and casting, which are known to be very timely and costly due to the use of specialised materials [26, 27]. Available AM processes such as stereolithography (SLA), fused deposition modelling (FDM), polymer material jetting (PJT/MJT), selective deposition lamination (SDL), and laser object manufacturing (LOM) can be utilised to highlight such clinical phantoms with patient-specific dimensions at relatively low costs and rapid manufacturing lead-times.

In this paper, we discuss in detail the current clinical applications of AM in radiotherapy, focusing on commonly used radiotherapy tools such as bolus, anthropomorphic phantoms, immobilisers, compensators, and brachytherapy moulds. Key findings and future insights are discussed throughout this study involving past and current methodologies and how AM is integrated in the current day to day clinical practice in radiotherapy.

2. Radiation therapy overview

RT plays a significant role in the management and treatment of cancer. Significant research is directed towards the non-invasive use of external beam radiotherapy (EBRT) and their advanced and localised cancer treatment capabilities including stereotactic body ablative radiotherapy (SABR) and proton therapy. For invasive procedures, internal radiotherapy (IRT) utilises invasive surgical procedures and seed implementation (brachytherapy) where radioactive seeds are directly implanted adjacent to cancerous cells.

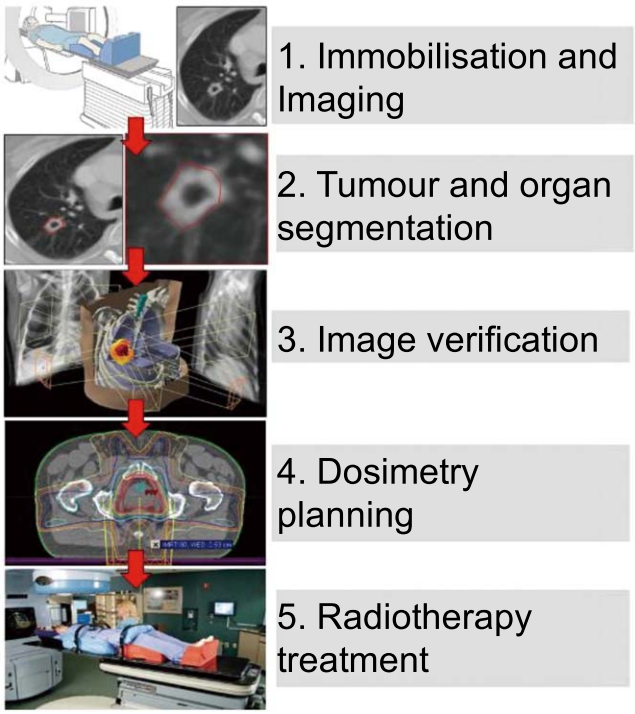

Figure 1. Common clinical workflow of external beam radiation therapy process (EBRT).

The common EBRT pathway is illustrated in figure 1 and consists of the following steps: (1) patient immobilization and imaging with modalities ranging from computed tomography (CT), magnetic resonance imaging (MRI), positron emission tomography (PET), single-photon emission computed tomography (SPECT), ultrasound or through simple x-ray radiographs; (2), (3) followed by tumour segmentation where attending clinicians identify tumour volume parameters (i.e. shape and position) and margins considering critical structures prior to image validation procedures; (4) computerised treatment planning systems (TPS) are then utilised by clinicians and physicists to virtually simulate the radiotherapy process where dose beam directions and intensities are optimised for enhanced patient treatment. The optimisation can either be done by the operator who choses beam number, shape, directions and dose contribution (forward planning) or done using a computer algorithm, a process called inverse treatment planning. Once treatment plans are finalised and approved, the actual patient irradiation process is implemented where (5) the intended full dose is divided into small doses (fractions) and delivered to the patient in specified intervals (i.e. usually daily) to allow healthy tissues to recover between treatments.

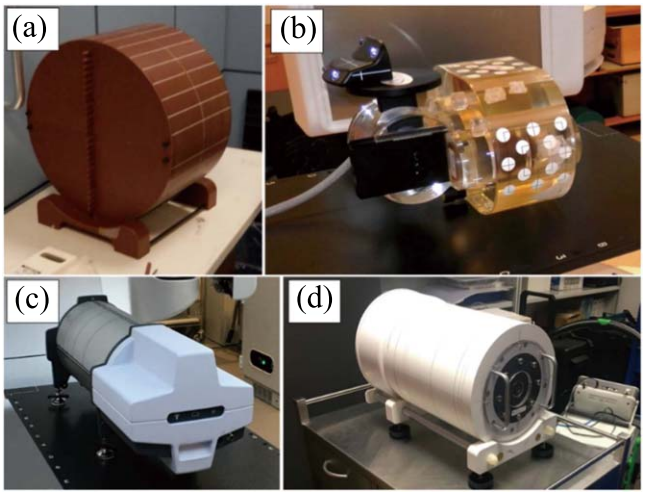

Figure 2. Dosimeter arrays used for patient specific QA: (a) TomoTherapy 'cheese phantom', (b) Modus QUASAR with motion insert, (c) ScandiDos Delta4, (d) SunNuclear ArcCheck.

2.1. Treatment planning process

The treatment planning process utilises computer algorithms, using TPS, to determine the best treatment parameters for the disease of the individual. These parameters include target volume(s), dose-limiting structures, dose prescription, dose fractionation, dose distribution, positioning of the patient, treatment machine settings, and adjuvant therapies. The system also produces reference images and other data which aid set-up and position verification of the patient in each treatment fraction. The final output of this process is then followed precisely by attending clinicians over several weeks [28].

2.2. Radiotherapy quality assurance

Given the high and potentially dangerous doses of radiation given to patients, quality assurance (QA) is an essential part of radiotherapy practice [29, 30]. In several clinical trials, the importance of high-quality delivery has been demonstrated [31] with technical QA typically assessing both dose delivered and the geometric precision of the delivery. QA processes of radiotherapy delivery can be commonly divided into two parts, the validation of a process in a generic phantom or the verification of dose delivered in a delivery sequence for an individual patient. The problem with both is that they typically employ a standard representation of a human patient, as illustrated in figure 5.

For the end-to-end testing of a new procedure, anthropomorphic phantoms are commonly used. They mimic the radiation properties of a standard patient. While paediatric size phantoms are available, the largest size of phantom mimics a small normal-weight healthy male. None of the commercial phantoms represents an obese patient or includes pathology such as tumours, emphysematous lungs or metallic hip replacements. The same applies to patient-specific QA, where the radiotherapy plan developed for an individual patient is delivered onto a detector array that usually is a Perspex cylinder of human dimensions (see figure 2). If the measurement that can easily be taken in the phantom compares well with the treatment plan, it is assumed that the dose distribution calculated for the patient using the same algorithms is also correct.

AM allows us to address both of these shortcomings. It can create realistic phantoms (or modify existing ones) that can mimic real patients with co-morbidities, different shape lesions and a variety of different body shapes. Similarly, AI can create phantoms that can represent the complexities of real humans adequately providing for more meaningful QA for individual patients.

2.3. Considerations for AM design

AM provides designers with potential to extend their capabilities into highly accurate patient-specific models [1]. There are technological and material specific constraints that apply when designing for AM. To help identify which of these constraints apply to your product design, the appropriate AM technology needs to be selected for the intended use. Computed aided drawing (CAD) is an essential component of the design process in any AM product. The complexity and quality of the product design is dependent on the skill of the CAD designer. The constraints are defined by the build angle tolerance of the printer and the orientation which impacts the mechanical properties of the product. Layer thickness varies with the different AM technologies. Print orientation will affect the duration of the build and in some cases the quality of the product. All these constraints will influence the final product and its manufacturability.

3. Advances in AM for radiation oncology

A patent from the Leland Stanford Junior University briefly discussed the familiarity of their inverse planning method for radiosurgery with the very first three-dimensional AM techniques, SLA, where ultra-violet beams solidify liquid resins in such a way that a particular shape is obtained [32]. AM in Radiotherapy was soon conceptualised by Ju *et al* [33], illustrating its feasibility in manufacturing low-cost proton range compensators which were found to have comparable dosimetric and density results with conventional compensators manufactured through computerised milling machines (CMM). Since then, interests in AM have extended towards the use of personalised bolus devices [34, 35], which are now part of the day-to-day clinical work for some radiotherapy centres. Active research is also currently being implemented for the AM of patient-specific radiotherapy phantoms [36], immobilisation devices [37], and brachytherapy moulds [38].

3.1. Bolus

Clinically used bolus devices are moulded thermoplastics sheets with tissue-equivalent properties to modulate the dose received by the patient's skin. Compared to standard wedge filters which are placed close to the radiation source (treatment head), boluses are placed directly on the patient's skin.

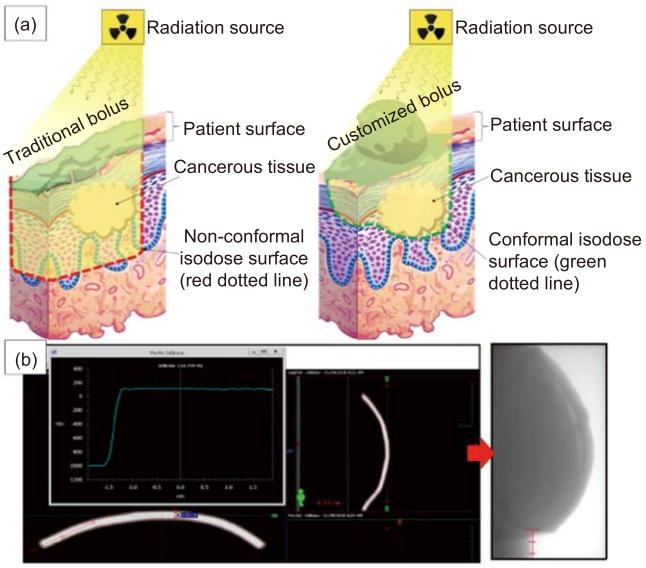

Figure 3. (a) Schematic diagram of observed skin isodose from traditional bolus compared with customised bolus manufactured through the AM process and (b) CT view of printed breast bolus on patient.

Common tissue-equivalent materials for bolus manufacture include superflab, aquaplast, and superflex (see figures 4(a) and (c) (top)) and are categorised into pliable or rigid forms where: pliable boluses conform with patient skin surface at given thicknesses, and rigid boluses are usually implemented for smaller regions not requiring compliance with patient's skin. However, inherent limitations of standard bolus devices include insufficient contact with patient's skin (i.e. nose, ear, and scalp), leading to air gaps and a reduction in both the maximum and surface dose [39], further leading to inadequate treatment of superficial lesions.

Recent developments in AM-bolus devices include the use of the FDM printing process [40–42], which is the extrusion process of thermoplastics layer-by-layer [43]. This process allows the fabrication of geometries conforming to irregular surfaces (i.e. nose, chest, etc) with controlled thickness values to provide better dose coverage compared to traditional flat bolus sheets (see figures 3(a) and (b)).

Common filament materials for AM-bolus include acrylonitrile butadiene styrene (ABS) [34, 44] and polylactic-acid (PLA) [45, 46]. Due to non-toxicity and biocompatibility with comparable treatment planning system (TPS) dose profiles, PLA is currently preferred by clinicians for clinical bolus use [47]. The use of flexible material such as thermoplastic polyurethane (TPU) is also being investigated for their improved compliance and reduced air gaps for patient comfortability [48, 49]. A recent release of flexible (soft) PLA may be able to highlight both patient skin conformity and tissue-dose equivalence [50].

3.2. Compensators

Compensator devices are fabricated using the moulding and casting process followed by milling, utilising solid water [51], lead [52], tungsten [53], or woods metal (cerrobend) [54] materials for megavoltage x-ray radiotherapy. Similar to wedge filters, these devices are attached close to the primary beam to attenuate beam dose with insignificant effects towards dose scattering within the patient [55]. Significant factors to be considered in manufacturing these devices include the field size, beam energy, and depth of the point of interest as they determine the required compensator thickness for treatment. These factors require personalised moulds, which are often expensive due to the fabrication process and materials involved. With the AM process, the fabrication of compensator devices not only reduces costs and manufacturing time but also enable the development of more complex geometries for beam attenuation [56, 57] (see figure 4(d)). The early literature of 3D printed compensators includes compensator blocks [58] and proton-range compensators [33, 59] (see figure 4(e)).

3.3. Anthropomorphic phantoms

Commercially available anthropomorphic phantoms are utilised for quality assurance purposes (see figures 5(a)–(d)) [60–63], for instance, the commissioning of new treatment procedures/machines or the validation of patient treatment plans using dose measurement tools such as thermoluminiscent dosimeters (TLD), dosimetry films, and ionisation chambers. Unfortunately, these phantoms do not fully represent patient-specific anatomies and pathological features, leading to unaccounted dose errors. More recently, review studies regarding AM of radiotherapy phantoms include the AM of imaging and dosimetry phantoms [64] and the varying imaging modalities used for AM-phantoms such as CT, MRI, PET, SPECT, and ultrasound [65]. Both studies have shown the feasibility of utilising inexpensive printing machines in particular for the FDM process to fabricate printable patient-specific geometries from patient imaging data.

Similar to the AM-bolus devices, common printing filaments used for AM-phantoms include standard materials from PLA and ABS, to specialty filaments from TPU, high-impact polystyrene (HIPS) and polymethyl methacrylate (PMMA). The main objective of AM-phantoms is to mimic patient-specific human tissue in terms of (a) imaging attenuations, for instance Hounsfield units (HUs) in CT and (b) dosimetric attenuations considering Compton effects in radiotherapy where electron density and atomic composition of the associated printing materials are both key factors for tissue mimicry within the radiotherapy setting (see figures 5(e)–(h)) [66–69].

Workflow for AM-phantoms initiates from (1) utilising patient CT, (2) the segmentation process of region of interests (i.e. lung tissue, bone, soft tissues), (3) 3D-model generation of segmented regions, post-processing, and printing parameter modifications and finally, (4) the FDM printing process of sliced models, assembly of printed models and the final implementation for imaging or dosimetry work (see figure 6). Other printing technologies utilised for AM-phantom fabrication also include PJT/MJT which allows multi-material and deformable material printing [66, 70, 71] and paper-based 3D printing utilising LOM and SDL processes [72, 73].

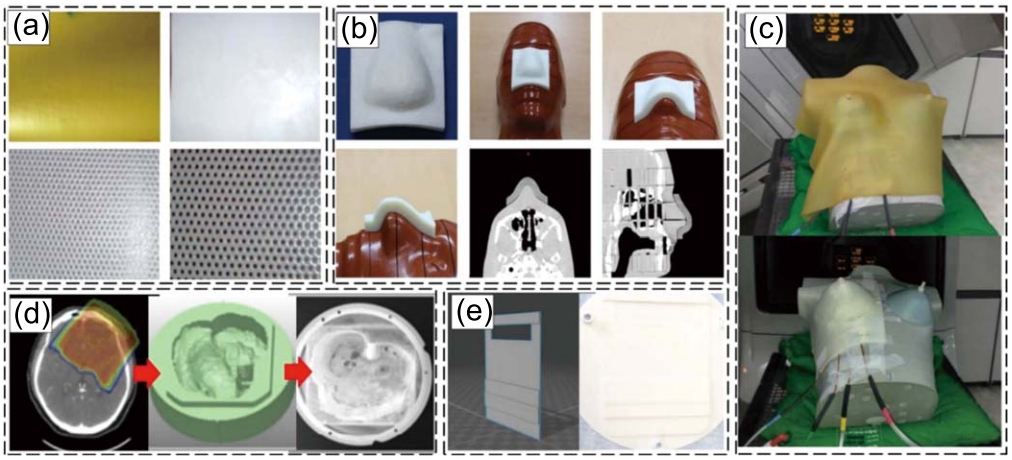

Figure 4. (a) Varying tissue-equivalent bolus materials for moulding including superflab, solid Aquaplast, fine mesh Aquaplast and large mesh Aquaplast [20], (b) FDM printed ABS nose bolus on the RANDO phantom [34], (c) comparison between (top) a superflex bolus and (bottom) a 3D printed PLA phantom specific bolus [45], (d) manufacturing a range compensator from STL generation to printing, and (e) a compensator device fabricated through 3D printed compensator mould filled with wax and tungsten powder. (d) Reprinted from [33], Copyright 2014, with permission from Elsevier. (e) Reproduced with permission from [56]. © 2016 American Association of Physicists in Medicine.

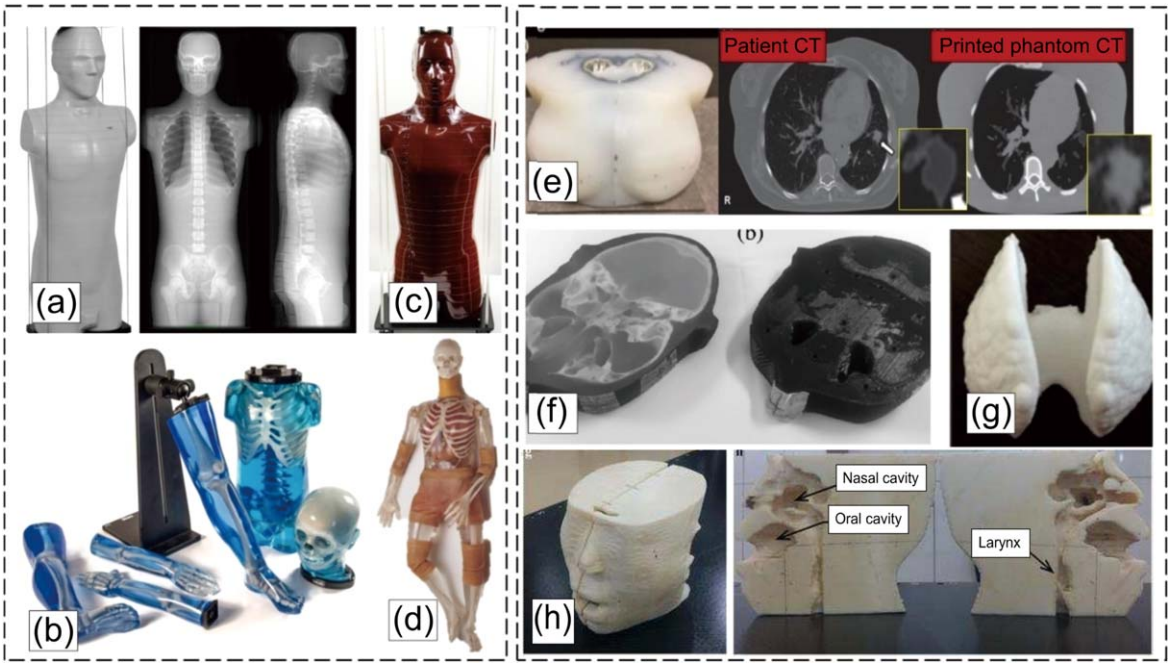

Figure 5. Illustration of commercially available anthropomorphic phantoms: (a) ATOM® CIRS Adult phantom and associated x-ray images [60], (b) SPoRT Paediatric CIRS phantom kit [61], (c) Alderson adult phantom [62], (d) RSD Pixy phantom [63], and patient-specific phantoms manufactured through 3D-printing: (e) patient-specific thorax phantom with 3D-printed bone and lung regions (silicone thorax body) and CT comparison of lesions between patient and phantom data, (f) an image of a standard head phantom slice and its 3D-printed version using FDM printing, (g) a 3D-printed thyroid phantom, and (h) a head phantom slice illustrating internal nasal—oral cavities and Larynx. (e) Reproduced with permission from [66]. © American Aossication of Physicists in Medicine. (f) Reprinted from [67], Copyright 2017, with permission from Associazione Italiana di Fisica Medica. Published by Elsevier Ltd. (g) Reprinted from [68], Copyright 2017, with permission from Elsevier. (h) Reproduced from [69]. CC BY 4.0.

The following selected methodologies further highlight innovative AM research associated with the fabrication of anthropomorphic phantom models:

- Nowak *et al* [74] developed an open-source software to accommodate the rapid conversion of contours from DICOM CT data to printable models and which can be extended towards other applications such as bolus devices.
- Leary *et al* [75] developed a method to convert CT DICOM data to fabricate bi-modal head phantom slice using polymer material jetting technology.
- Leary *et al* [76] demonstrated the feasibility of modulating phantom HUs using one printing material by utilising engineered square voids and its effects on CT imaging, known as the partial volume effect (PVE).

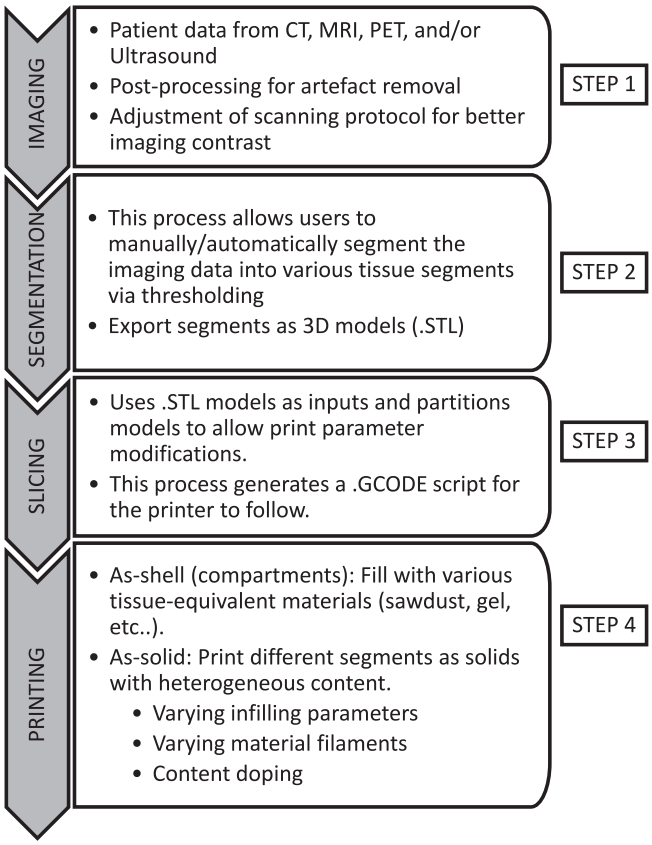

Figure 6. The standard AM workflow for the fabrication of radiotherapy phantoms: (1) patient CT image input, (2) segmentation region(s) of interest, (3) slicing segmented 3D models, and (4) printing process. Reproduced with permission from [64].

- Tino *et al* [77] utilised porosity of Gyroid structures to further modulate the observed Hounsfield numbers of phantoms.
- Okkalidis *et al* [78] developed a technique to modulate HUs of a single printing material by controlling material extrusion rate.
- Irnstorfer *et al* [79] demonstrated a proof-of-concept in neonatal radiotherapy using acquired x-ray attenuation patterns.
- Yoon *et al* [80] have demonstrated the feasibility of a 3D printed lung phantom with printed lung lesions for stereotactic lung study using a motion platform device to simulate realistic lung movements (QUASAR, Modus Medical Devices, Canada).
- Jahnke *et al* [72, 73] have demonstrated the feasibility of fabricating realistic head phantom models through (1) a paper-based 3D printing method and (2) a customised LOM printer where it utilises a toner from the laser printer to act as an adhesive to stack all printed sheets. This application shows promising results however, as this application is still new, CT tissue-equivalence (HU) and dosimetry are yet to be quantifiable further research must be conducted regarding reproducibility.

3.4. Immobilisers

When previously discussed constraints (section 2.3) are combined into a clinical environment, another level of complexity is realised. The main clinical implications relate to the level of patient comfort, the rigidity of the product to provide the correct level of immobilisation and the suitability of the product design for individual patients [20, 22] and the response of material to irradiation in terms of degradation and attenuation. Immobilising tools in radiotherapy are utilised by clinicians to accurately position and rigidly immobilise patients prior to treatment. Common immobilisation devices include beaded bags [81, 82], polyurethane foam castings [83–92], orthopaedic plastics [93–96], head masks/holders with bite blocks [97] or without [98] using thermoplastics [99] (see table 1). Current limitations of standard immobilising techniques were observed to cause mental and physical distress towards patients ranging from anxiety to physical discomfort and claustrophobia [100–103].

Utilising AM, fabrication of immobilising devices highlights personalised and customisable geometries achievable through the AM modelling and printing process [31, 37, 104, 105]. The fabrication process of these devices follows a similar pathway for all 3D printed radiotherapy devices initialising from CT data, to model processing and generating a printable 3D model and finally, printing [106] (see figure 7). The other pathway to develop printable models utilises surface laser scanners for generating reference models for constructing immobilising shells [107, 108].

Furthermore, AM-immobilisers in the literature utilise a range of printing techniques including FDM, SLA, SLS, and PJT/MJT with extensive work regarding materials focusing on mechanical and imaging properties [108, 109], with both PLA and ABS a common printing material. Other than the general head and neck 3D printed immobilisation devices [106, 110] (see figures 7 and 8, respectively), segments suited for immobilisation also include abdominal area [111], the mouth [112] and breasts [113].

3.5. Brachytherapy moulds

Brachytherapy (a form of radiation therapy using an internal radiation source) can provide highly conformal radiation dose distribution to a targeted lesion. Brachytherapy mould is often used for nonmelanoma skin lesions that usually involve irregular surface, requiring a customised mould to fit along the surface (see figures 4(b) and (c)). Available data confirm that brachytherapy is an efficient and well-tolerated treatment that offers excellent cosmesis and low toxicity for skin cancer patients [114, 115]. Conventional methods to construct a customised mould include using specialised polymers, acrylic resin, wax (similar to dental wax) or a thermoplastic material or similar [116, 117]. Commercial flap applicators, which can be prefabricated with the desired geometry, are also being clinically used. Such commercial solutions include the Freiburg flap (Elekta), the H A M (Mick Radio-Nuclear Instruments), and the Catheter Flap set (Varian Medical Systems).

Table 1. Immobilisation capabilities. Reproduced from [22]. Copyright 1995, with permission from Elsevier.

Site	Technique	Treatment to treatment	Simulation to treatment	Alignment
Pelvis/abdomen	Alpha-cradle or thermoplastic casts	3–4 mm	6 mm	Laser
	Unimmobilised	6–8 mm		Laser
Breast	Alpha-cradle or vacuum bead bags	3 mm		Light field
Thorax	Unimmobilised	4 mm	6 mm	Laser
Head/neck	Face masks w/neck	2.5–4 mm		Laser
	Mechanical	3 mm	2.5 mm	Laser
	Bite block	4 mm	6 mm	Laser
Intracranial	Unimmobilised	3 mm	5 mm	Laser
	Face mask w/neck	2–2.5 mm	*	Laser
	Cranial fixation (stereotactic)	<1 mm	*	Mechanical
	Non-invasive (stereotactic)	1–1.5 mm	*	Mechanical

*not specified.

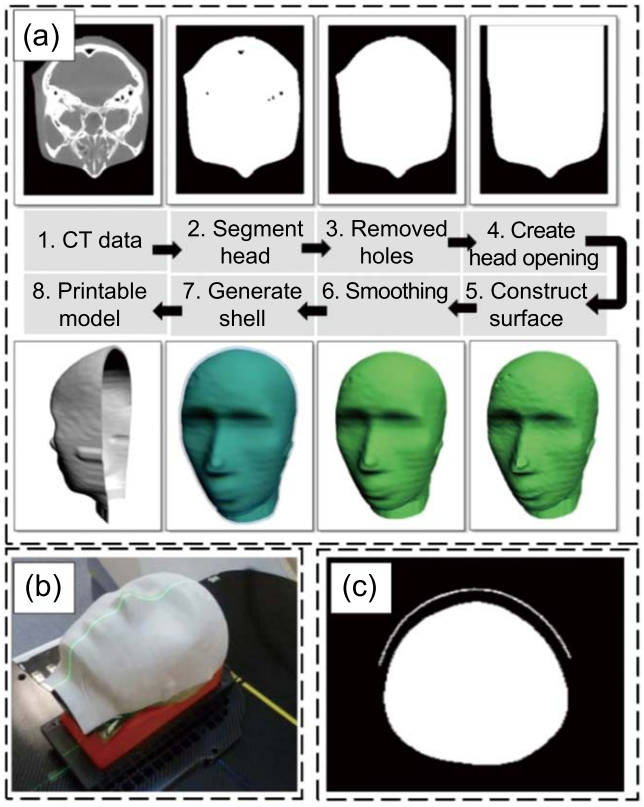

Figure 7. (a) Mask generation workflow from CT data, (b) rescanned phantom fitted with the printed mask, and (c) a single binarised CT slice from scanned phantom with printed mask. Reproduced from [106]. CC BY 4.0.

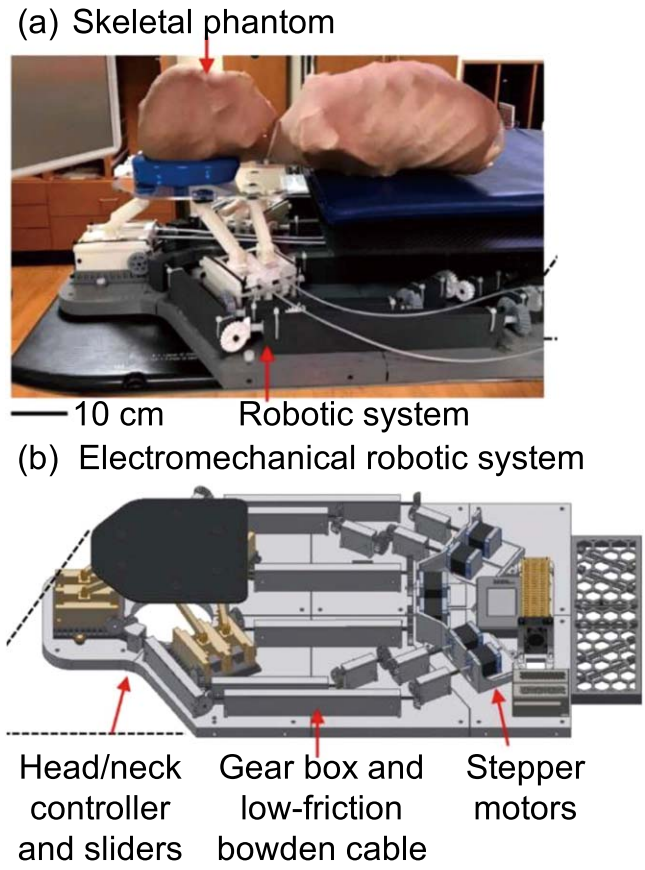

Figure 8. (a) A skeletal phantom on a 3D printed additional head and neck immobilisation frame, added on an existing treatment couch and (b) schematic illustration of the robotic system. Reproduced from [110]. CC BY 4.0.

These applicators can be cut to any size to fit the target area, however, this may result in an air-gap when not perfectly fitting, in particular for irregular and large skin lesions.

AM can play an important role here to offer better well-fitting personalised AM-moulds than the aforementioned conventional approaches. An increasing number of studies have demonstrated the application of additive manufacturing in skin brachytherapy domain, and its feasibility studies show promising results [118, 119]. There is still more work to be done to ensure skin moulds can accurately model dosimetric calculation for radiotherapy. Current literature in AM-radiotherapy (2019–2020) are summarised in table 2. Capabilities of AM technologies regarding HU-equivalence are also summarised in table 3.

4. Opportunities and future direction of AM in radiation oncology

Radiotherapy is leaning towards bespoke models to accommodate the advancing diagnostic and treatment technologies

Table 2. A summary of recent available AM-radiotherapy literature as of 2019–2020.

Authors	Target body segment(s)	AM technology	AM model(s)	AM material(s)	Input modality	References
			BOLUS			
Baltz *et al*	Scalp	PJT/MJT	Stratasys J750	Agilus (60 shore hardness)	CT	[120]
Kong *et al*	Nose	FDM	MakerBot Replicator II	PLA	CT	[121]
Park *et al*	Head	FDM	Zortrax M300	TPU (NinjaFlex)	CT	[49]
Sasaki *et al*	Nose, scalp, ear, knee, Tibia, lacrimal gland	FDM	MakerGear M2 s	PLA	CT	[122]
An *et al*	Breast	FDM	Zortrax M300	HIPS	CT	[123]
			ANTHROPOMORPHIC PHANTOM			
Bustillo *et al*	Thorax	FDM	**	ABS, PLA	CT	[124]
Kadoya *et al*	Head and Neck	FDM	**	ABS, PLA	CT	[125]
Zhang *et al*	Lung	FDM	**	ABS, modified resin	CT	[126]
Niebuhr *et al*	Pelvis	PJT/MJT	Objet 30 (Stratasys)	Veroclear	CT	[127]
Makris *et al*	Head	PJT/MJT	Projet 360 (3D Systems)	*	CT	[128]
Price *et al*	Liver, spleen, kidney	*	*	Acrylic-based photopolymer	CT	[129]
Irnstorfer *et al*	Thorax (neonate)	SLA, FDM	Form 2 (Formlabs), Ultimaker 2+	*	CT	[79]
He *et al*	Breast	MJT, FDM	Objet 50, **	***, ABS	Mammography, MRI, Ultrasound	[130]
Hernandez-Giron et al	Lung	PJT/MJT	Projet printer	VisiJet EX200	CT	[70]
Jahnke *et al*	Head	LOM, SDL	Customised LOM, Mcor IRIS 3D Printer (Mcor)	*	CT	[72]
Wood *et al*	Head	SLA	Stratasys printer	DSM Somos WaterShed XC 11122	MRI	[131]
Grehn *et al*	Head	FDM	**	*	CT	[132]
			IMMOBILIZERS			
Loja *et al*	Head	FDM	**	ABS, PMMA, PPS, PC	CT	[108]
Cardenas *et al*	Abdomen	FDM	**	PLA	CT	[111]
Burns *et al*	Breast	FDM	uPrint	ABS	CT	[113]
Kitamori *et al*	Head and Neck	PJT/MJT	*	*	CT	[112]
Ostyn *et al*	Head and Neck	PJT/MJT, FDM	Objet Eden 260VS, uPrint, Makerbot Z18	PLA, ABS, Verowhite Plus	CT	[110]
			BRACHYTHERAPY MOULDS (with catheters)			
Lancellotta *et al*	Mouth	SLA	Formlabs printer	Dental SG Resin	CT	[133]
Casey *et al*	Left anterior shin	PJT/MJT	Projet 2500 Plus (3D Systems)	VisiJet M2 ENT	CT	[134]
Bassi *et al*	CIRS Anthropomorphic phantom	FDM	**	TPU materials (NinjaFlex, Wolfblend, Cheetah)	CT	[135]
Park *et al*	Superficial skin	FDM	**	HIPS	CT	[136]
			BRACHYTHERAPY MOULDS (with catheters)			
Chmura *et al*	Superficial skin	FDM, SLA	Creality 10 (CR-10), Form 2	PLA, ****	CT	[137]
D'Alimonte *et al*	Penile surface	FDM	**	*	CT	[138]
Imber *et al*	Head	FDM	**	*	CT	[139]

Table 2. (Continued.)

Authors	Target body segment(s)	AM technology	AM model(s)	AM material(s)	Input modality	References
Zhao *et al*	Vaginal applicator	FDM	Replicator + (Makerbot)	PLA	CT	[140]
Taggar *et al*	Fingers	SLA	*	Clearview resin	CT	[141]
Laan *et al*	Vaginal applicator	DLP	Perfactory 4 mini XL (Envisiontec)	R5 resin	MRI	[118]

Note. No recent literature on 3D printed compensator devices exists, thus they are not included in this table.
Abbreviations: PJT, polymer jetting technology; MJT, material jetting technology; FDM, fused deposition modelling; SLA, stereolithography; DLP, digital light processing; LOM, laminated object manufacturing; SDL, selective deposition lamination; PLA, polyactic acid; ABS, acrylonitrile butadiene styrene; PMMA, polymethyl methacrylate; PPS, polyphenylene sulphide; PC, polycarbonate; HIPS, high-impact polystyrene; TPU, thermoplastic urethane; MRI, magnetic resonance imaging; CT, computed tomography.
*not specified, **FDM printer not specified, ***MJT material not specified, ****SLA material not specified.

Table 3. Common AM materials used for radiotherapy phantoms, their specifications, and their achievable HUs in standard CT protocol. Adapted from [64].

Material	Cost (USD)	Physical density (g cm^{-3})	Achievable HUs		Suitable HU-equivalence
			Solid	Modified infill	
Fused deposition modelling (FDM)—≈178–330 μm layer thickness					
PLA	≈20 to ≈ 30 per kg	≈1.24	≈20 ⩾ HU ⩽ ≈200	≈−950 ⩾ HU < ≈0	L, WM, GM, B, M, K, CSF, F, W, LT, CB1, T, S
ABS	≈20 to ≈ 30 per kg	≈1.08	≈−100 ⩾ HU ⩽ ≈50	≈−900 ⩾ HU < ≈10	L, WM, GM, B, M, K, CSF, F, W, LT, T, S
ABS doped with barium sulfate/ bismuth	—	—	HU > 1000	*	CB2
HIPS	≈30 to ≈ 40 per kg	≈1.08	≈−280	≈−800 ⩾ HU < ≈−450	F, LT
PC	≈75 to ≈ 90 per kg	≈1.18	≈−15	*	F
TPU (flexible)	≈30 to ≈ 40 per kg	≈1.40	≈10 ⩾ HU ⩽ ≈180	*	L, WM, GM, B, M, K, CF, T, S
Metallic composites	≈30 to ≈ 100 per kg	≈1.80 to ≈2.30+	≈100 to ≈ 8000+	*	CB,
Stereolithography (SLA)—≈50–125 μm layer thickness					
VisiJet line	≈400 per litre	≈1.04	≈150	*	L, M, T
Digital light printing (DLP)—≈5 μm layer thickness					
Standard resin	≈80 to ≈ 150 per litre	≈1.04	≈152	*	L, M, T
Selective laser sintering (SLS)—≈80–150 μm layer thickness					
Nylon	≈45 to ≈ 75 per kg	≈0.93	≈−500	*	LT
Binder jetting (BJ)—≈200 μm layer thickness					
Gypsum	≈3 per kg	≈2.90	≈750	*	CB1
Polymer jetting technology (PJT)/ Material jetting technology (MJT)—≈16–30 μm (1600–850 dpi) layer thickness					
SUP705 Support material	≈200 per kg	≈1.12	≈90	*	L, M, T
TangoBlack Plus line	≈400 per kg	≈1.12	≈100	*	L, M, T
VeroWhite and VeroBlack	≈300 per kg	≈1.17	≈110	≈−870 ⩾ HU ⩽ ≈110	L, M, T
VeroClear	≈350 per kg	≈1.18	≈120	*	L, M, T
Agilus, 27–70 shore hardness	≈370 per kg	≈1.14	≈40 ⩾ HU ⩽ ≈80	*	L, WM, GM, B, M, K, T

* not specified.

Abbreviations: L, liver; WM, white matter; GM, grey matter; B, blood; M, muscle; K, kidney; S, spleen; CSF, cerebrospinal fluid; F, fat; W, water; LT, lung tissue; CB1, cancellous bone; CB2, cortical bone; T, tumour.

such as the use of high precision stereotactic radiosurgery and proton therapy in allowing the full potential of personalised radiotherapy. Recent work by the Association of University Radiologists Radiology Research Alliance (AUR-RRA) task force on 3-dimensional printing has published two separate papers investigating the logistics of clinical translation using the 3D printing technology in radiotherapy [142] and a more comprehensive insight towards the clinical applications of 3D printing in radiotherapy [143].

The following sections focus on significant research opportunities at the interface between radiotherapy and AM.

4.1. Generative design for medical additive manufacturing

Additive manufacture enables the design of high-complexity bespoke structures that are eminently compatible with the requirements of medical radiotherapy applications, including the bolus devices, compensators, phantoms, immobilisers and brachytherapy moulds reviewed in this work. Despite the opportunities for enhanced medical outcomes enabled by these technologies, the ability of a human designer to manually accommodate the complexity inherent to such design is limited. Consequently, AM-medical applications are potentially subject to high cost due to manual design and error checking effort, as well as regulatory challenges associated with confirming the suitability of this manually generated design.

4.1.1. Introduction to generative design systems. In response to these challenges, generative design (GD) systems are emerging within the AM community to enable the low-cost design of high-complexity systems, such as patient-specific medical systems. In broad terms, GD systems refer to 'the rules for generating form, rather than the forms themselves' [144]. In *Creative Evolutionary Systems*, GD tools enable design decision making and reporting to occur with the speed and repeatability of the available computational resources, rather than requiring manual decision making, thereby enabling design outcomes that are practically unachievable by a human designer.

A schematic representation of a GD system is provided in figure 9, including phases of problem, where the technical and oncological design requirements are formally specified; embodiment design, consisting of the generation and evaluation of high-level solutions to the problem definition; and detail design, where the specific solution is formally defined to enable manufacture [145]. In GD design, a generative design system algorithmically replaces one or more of these identified design phases.

In order to provide a useful design for additive manufacturing (DFAM) outcomes, the generative design system must replace one or both of the embodiment or detail design phases. For medical oncology applications, it is likely that the AM and oncological subject matter experts would agree on a preferred embodiment based on their subject-matter expertise, but that the detail design phase be applied with a GD system such that patient-specific design outcomes can be algorithmically generated.

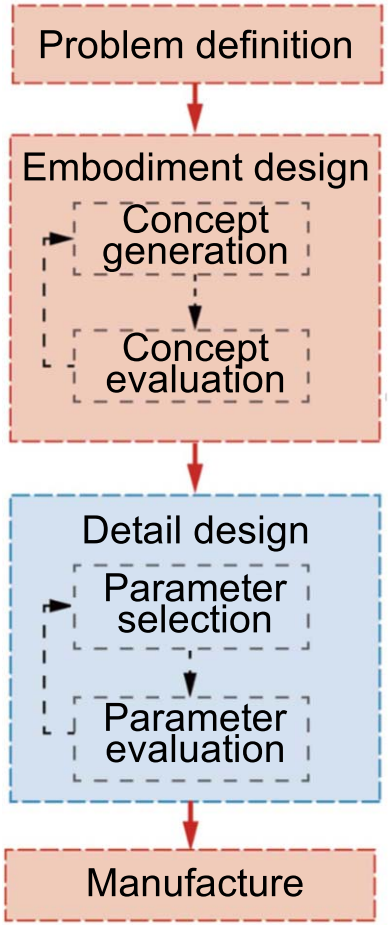

Figure 9. A simplified schematic of the formal design process as relevant to GD. The blue highlighted design phases are typically implemented as GD systems for medical applications.

4.1.2. Application of GD systems for oncological application. GD outcomes are particularly important for high-value AM product that is customised to the specific requirements of a particular oncological scenario. This methodology has been applied in the design and manufacture of patient-specific radiotherapy phantoms based on observations associated with the partial volume effect (PVE); which allows local values of the phantom HU to be tuned by geometrically manipulating the local phantom geometry [76]. This method thereby allows the rapid manufacture of patient-specific phantoms based entirely on algorithmic manipulation of (see figure 10) the patient CT data, resulting in a locally defined density field, that is then converted to an AM data input file for manufacture. This methodology enables low-cost deployment of high-value oncological products according to the patient-specific requirements, as well as providing certification documentation as required for medical manufacture.

4.2. Water-tight and multi-material 3D printing

Material extrusion printers (FDM) are gaining greater attention due to new developments in printable materials and novel methodologies with reduced manufacturing costs and time

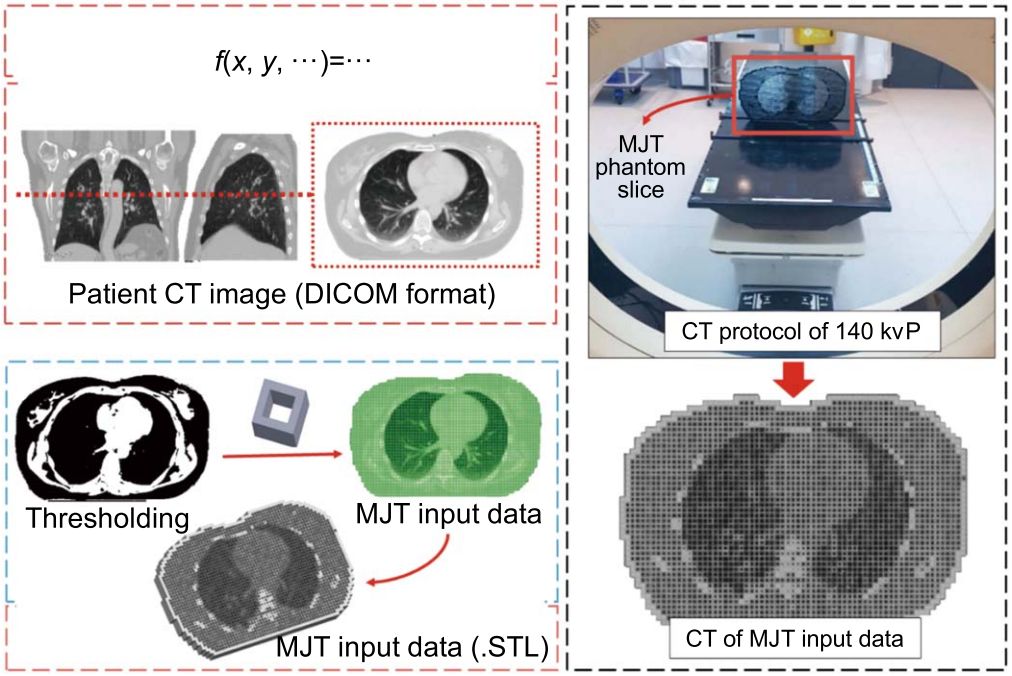

Figure 10. GD system applied for algorithmic following schematic in figure 9 to generate a patient-specific radiotherapy imaging phantom using material jetting technology (MJT). Reproduced with permission from [76]. Copyright © 2020 by ASME.

with comparable printing resolutions to high-end printers such as PJT/MJT and SLA. For example, fabricating water-tight devices requiring high-resolution printing as close to 25-micron layer height, may require the use of the SLA technology, which uses a UV-curing process to polymerise liquid resins for microchannel fabrication [146] or the fabrication of a head phantom with fillable compartments using tissue-like liquids for magnetic resonance imaging applications [147] (see figures 11(a) and (b)). However, low-cost FDM printers may also be utilised for such applications as users can modify a huge range of printing parameters to achieve water-tight parts with comparable results to polymer jetting and SLA systems with high-resolution printing [148, 149]. Relatively low-cost FDM printers with high-resolution and multi-material printing capabilities are tabulated in table 4.

A very recent research paper published by Skylar-Scott *et al* [150], have demonstrated a novel fabrication technique of multi-material FDM printers (multi-material multi-nozzle 3D printing, MM3D) which enables rapid material extrusion using nozzle numbers as high as 128 (16 × 8 nozzles) with capabilities in printing deformable materials (see figure 11(c)). This significant advancement in the FDM technology not only raises the possibility of ultra-rapid 3D printing but also has importance in terms of heterogeneous tissue printing where varying tissue-like print filaments can be printed simultaneously for the patient-specific fabrication of radiotherapy phantoms and tissue-engineering applications. Unfortunately, new technologies as such will still need some validation in terms of material compatibilities, part manufacturability, and their significance in the clinical workflow.

Moving on to commercially available high-end multi-material printer such as the Stratasys J750 (Stratasys, US). The J750 printer uses the PJT/MJT process which utilises the UV-curing process to polymerise two or more photopolymer resins extruded in tiny droplets. Available materials for this printer include Agilus30, ABS, RGD720, Tango, Vero, VeroClear and VeroFlex materials. Varying material ratio combinations between different materials can produce multi-coloured parts with certain degrees of material flexibility (shore hardness).

Recent PJT/MJT applications to radiotherapy involve a mobile thorax phantom for 4DCT [71] and a mouse phantom for dosimetry [151]. Another printing methodology enabled by the J750 printer apart from multi-material printing involves the voxel printing technology which ignores the use of 3D model inputs for printing (i.e. STL, STP, 3MF, etc) and directly use RGB or BMP image stacks as inputs. This process, however, requires image pre-processing from image resizing and masking to image dithering [152]. The voxel method not only is a faster printing alternative as it bypasses the 3D model generation process but also provides better representation and material diffusion of heterogeneous structures from medical DICOM images for surgical guide model fabrication [153] (see figure 11(d)). With new proprietary tissue-like materials released by Stratasys [154] including: GelMatrix™ support resin for easy removal in printed narrow blood vessels, TissueMatrix™ resin for heart tissue fabrication and BoneMatrix™ resin for bone, voxel printing may be able to extend towards the fabrication of heterogeneous patient-specific phantoms directly from patient DICOM images. However, printed phantoms using this technology will still need various imaging and dosimetric studies to validate their manufacturability and tissue-like radiotherapy equivalence.

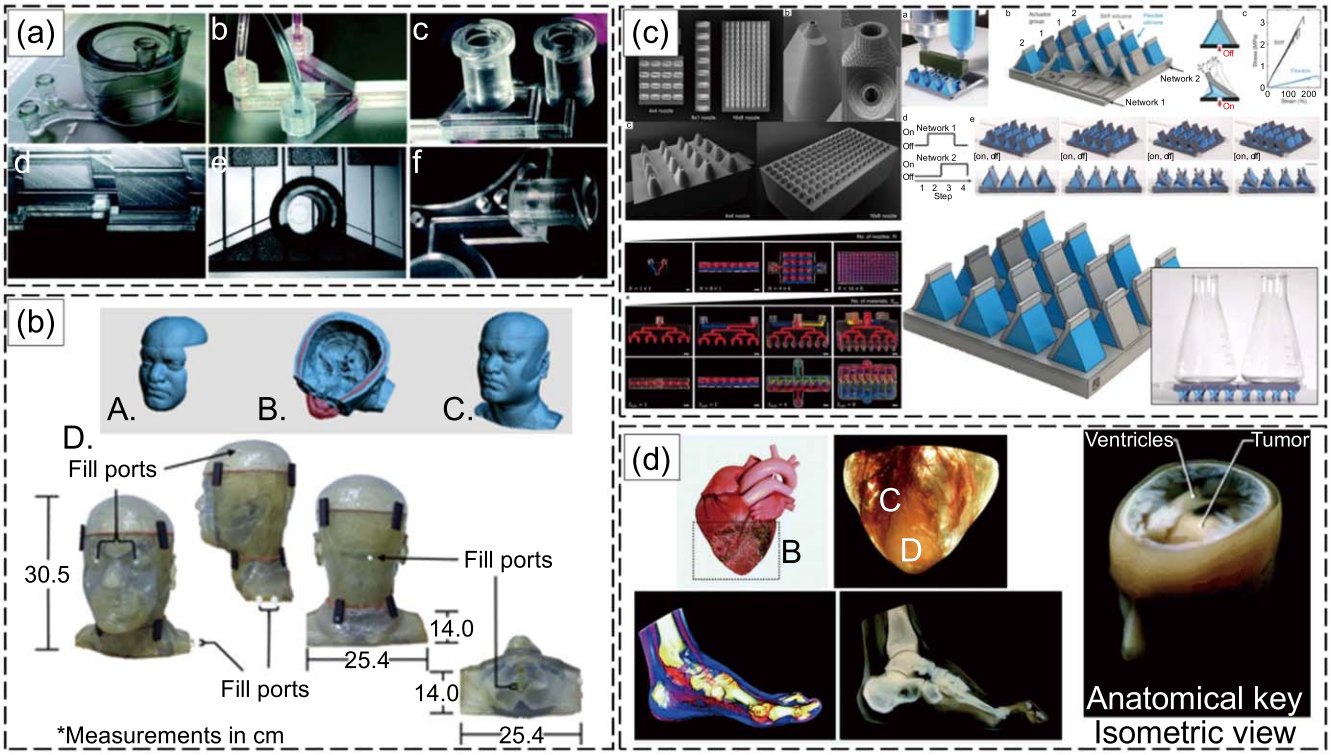

Figure 11. SLA fabrication of (a) microchannels, (b) fillable MR head phantom, (c) developing a soft robotic millipede walker module utilizing multimaterial multinozzle 3D printing technology (MM3D), and (d) using voxel printing technology to fabricate biomedical models. (a) Reproduced from [146] with permission of The Royal Society of Chemistry. (b) Reproduced from [147]. CC BY 4.0. (c) Reprinted by permission from Macmillan Publishers Ltd: Nature [150], Copyright 2019. (d) Reproduced with permission from [153]. Copyright 2018, Mary Ann Liebert, Inc.

Table 4. Available low-cost FDM printing machines with high-resolution and multi-material printing capabilities.

Name	Brand name	No. of printable materials in a single print job	Build volume (mm)
Prusa I3[b]	Prusa3D	5	250 × 210 × 210
Pallete 2 S[a]	Mosaic	4	—
Ultimaker S5	Ultimaker	2	330 × 240 × 300
Raise3D Pro 2	Raise3D	2	
Inventure	Zortrax	2	135 × 135 × 130
RoboxPRO	Cel	2	210 × 300 × 400
3DWOX 2X	Sindoh	2	228 × 200 × 300
M3-ID Rev 1	Makergear	2	180 × 254 × 203
Sigma R19	BCN3D	2	210 × 297 × 210
Craftbot 3	Craft	2	374 × 250 × 250
Flashforge Creator Pro	Flashforge	2	227 × 148 × 150
Geeetech A10M	GEEETECH	2	220 × 220 × 260
ZMorph VX	ZMORPH	2	250 × 235 × 165

[a] Add-on accessory for Ultimaker printers (Only for 2go, 2+, 2 EXT, 3,3 EXT).
[b] Requires Multi Material Upgrade 2 s (MMU2S).

4.3. Modular anthropomorphic AM-phantoms

The modularity of commercially available anthropomorphic phantoms is limited due to the manufacturing process of moulding and casting. For instance, horizontally sliced anthropomorphic phantoms such as the CIRS™ ATOM phantoms and the Alderson RANDO phantoms (ART) [25] only allow the insertion of TLDs and ionisation chambers with limited spaces for dosimetry films. Modularity in the phantom design highlights significant opportunities in 3D printing phantom slices with customised TLD and ionisation chamber insertion holes as well as placements for dosimetry films. Most AM-phantoms have demonstrated the feasibility of fabricating heterogeneous phantoms utilising different printing materials and technologies, with thorax phantoms consisting of patient-specific lesions [66, 71].

The reproducibility and modularity of AM-phantoms are key requirements for clinical use. However, the development

of modular phantoms allowing reproducible insertions of patient-specific segments (i.e. lesions, lung, soft tissues, bone), for varying patient treatment cases, is yet to be developed. A possibility to resolve this limitation is to utilise current GD systems in parallel with a range of AM technologies to design and fabricate inhomogeneous building blocks such as lesions, lung and soft tissues, and bone, much like LEGO®, to assemble a realistic phantom depending on a specific case for treatment planning.

4.4. 4D Phantoms

Precision radiotherapy relies on accurate conformal delivery of radiation, and one of the major challenges is the fact that organs move, squash and stretch in the abdomen regularly during breathing and due to organ filling and tumour response to treatment. The precision of modern radiotherapy techniques is limited by such anatomy changes, resulting in different spatial components of tumours and surrounding organs 'seeing' different radiation doses than that planned. Limitations as such will introduce discrepancies between planned and delivered radiation doses.

In this context, dynamically moving phantoms can add invaluable inputs on radiotherapy quality assurance throughout the process, imaging, planning, image verification and treatment [155]. Additive manufacturing can play a critical role here to construct more reliable, realistic, and cost-effective phantoms than limited commercial solutions, such as QUASAR™ (Modus Medical) CIRS dynamics (Varian Medical System) that simulate simplified anatomy motion.

An exciting application for AM 4D phantoms is to add a deformable feature in dynamic phantoms to better simulate deformably moving anatomy using AM technology. Until now, there is no solution in the commercial as well as research domains to emulate real patient-like anatomy change. AM has great potential to construct deformable structures that can emulate anatomy deformation. Such a phantom can be an invaluable tool to validate the mathematical modelling of anatomical deformation, where there is a lack of experimental data [71, 156].

4.5. Radiomic phantom models

Radiomics is based on the premise that important features of medical images are not necessarily perceivable by a human observer [157, 158]. These features can occur in several dimensions and pertain to shape of structures, texture, noise patterns and the relationship between neighbouring voxels of an image. Importantly radiomics features have shown to be related to tumour biology [159] and possibly clinical outcomes [160].

Radiomics features are usually extracted using computer analysis. They can be grouped and assessed using machine learning to link selected subsets of features to clinically relevant outcomes [161]. However, there is considerable variation in the quality of radiomics analysis between different institutions and validation of outcomes by independent observers is often difficult [159, 162].

It is important to develop test objects that mimic radiomics features in a predictable and reproducible fashion. Additive manufacture with its ability to modify object features in a systematic fashion appears to be a perfect tool to develop such objects [163]. One challenge is the required fine detail of resolution that is required to represent texture features of biological tissues. However, many groups are currently working on solutions to these issues, and it can be expected that the wide availability of such quality assurance and standardisation tools for radiomics will help to make the field more robust.

4.6. Open-source 3D model database for AM-radiotherapy devices

To further increase and promote the significance of AM in Radiotherapy, the growing clinical data on these 3D printed devices require the need for proper documentation and the development of open-source forums and databases including: generated 3D models from clinical data, their associated printing parameters, their imaging and dosimetry outputs. There may be an opportunity for developing such a global initiative for clinicians, especially for medical physicists and engineers, to validate printing methodologies prior to clinical use. The National Institutes of Health (NIH, US Department of Health and Human Services) have developed a database, known as NIH 3D Print Exchange consisting of 3D models related to bioscience and medicine where users can share their 3D models extracted from clinical patient CT data [164]. However, models used in this database are not intended for clinical use and are focused only in the visualisation and guidance for surgical procedures.

Another great initiative from the US, the 3D Printing Special Interest Group (SIG) formed by the Radiological Society of North America (RSNA), have established a 3D printing registry containing valuable data associated with clinical 3D printing and assistance with clinical decision making regarding the use of the AM. Current efforts have attracted major 3D printing companies such as Formlabs, HP, Materialise, and Stratasys to provide substantial support for further database development [165].

5. Summary and outlook

3D-printing is revolutionising the way clinicians approach the diagnostic and treatment stage of patients in radiotherapy. At present, the AM-radiotherapy field is in an exciting phase of exploration and innovation, evident by the increasing amount of research towards quality assurance of 3D printable materials, their limitations, and more importantly, their contributions to enhance the delivery of clinical patient treatments.

The following summary can be gained from this review:

- Over the years, the use of 3D printing in radiotherapy has sparked debates regarding implementation of AM fabricated phantoms for clinical use. The perspective that '3D printing technology will eventually eliminate the need for

purchasing commercial phantoms for clinical medical physics QA procedure' [166] is becoming more achievable as AM-radiotherapy phantoms advance towards faster, high-resolution and multi-material printing workflows with controllable deformability of materials. This also applies to other applications such as bolus, immobilizers, compensators, and brachytherapy moulds.

- Generative design is an emerging methodology for medical product design that enables commercial AM outcomes for scenarios that would be otherwise economically intractable, in particular, the manufacture of high-value patient-specific product at low cost and accommodating the requirements for certification documentation. The implementation of such GD systems provides a significant opportunity for enhanced patient outcomes; however, such systems should be implemented with reference to standard methods of medical system design such that verification and validation of the intended GD system are robustly implemented [167].
- Research directions for AM-radiotherapy applications must lean towards the development of new tissue-equivalent materials and structures through the FDM process to maintain low costs and print controllability. Other techniques include paper-based printing (LOM and SDL) to further simulate realistic CT imaging of tissues, although are still expensive and are yet to be validated for dosimetry work are used for training and optimisation for CT-guided procedures. Another alternative for improved printing of tissue-like components include bioprinting. However, similar to LOM and SDL, the associated printing and material costs are still very high compared to standard FDM printers. In addition, limitations observed from bioprinting in terms of parameterisation and vascularisation are yet to be solved and remain to be the biggest challenges in the bioprinting research field [168]. The FDM printing process remains to be the most commonly used printing method for AM-radiotherapy due to lower printing costs with relatively high-resolution and multi-material printing capabilities.
- For professionals (i.e. clinicians, physicists, and medical engineers) intending to use 3D printing for radiotherapy clinical use, extensive imaging and dosimetric assessments must be performed on printing material for their tissue-equivalence, considering inter- and intra-variabilities of outcomes. It is also recommended that proper documentation of clinically used 3D printed radiotherapy devices be implemented as it will play a significant role in providing guidance in future clinical AM-radiotherapy work, in particular for clinical regulations.

Acknowledgments

This research was conducted by the Australian Research Council Industrial Transformation Training Centre in Additive Biomanufacturing (IC160100026). The support of the Gross Foundation is also acknowledged.

ORCID iDs

Rance Tino https://orcid.org/0000-0003-4563-5491

References

[1] D'Urso P S 1998 Stereolithographic biomodelling in surgery *PhD Thesis* School of Medicine, The University of Queensland
[2] Pei X, Zhang B, Fan Y, Zhu X, Sun Y, Wang Q, Zhang X and Zhou C 2017 Bionic mechanical design of titanium bone tissue implants and 3D printing manufacture *Mater. Lett.* **208** 133–7
[3] de Moraes P H, Olate S, Cantín M, Assis A F, Santos E, Silva F O and Silva L O 2015 Anatomical reproducibility through 3D printing in cranio-maxillo-facial defects *Int. J. Morphol.* **33** 826–30
[4] Murr L E *et al* 2010 Next-generation biomedical implants using additive manufacturing of complex, cellular and functional mesh arrays *Phil. Trans.* A **368** 1999–2032
[5] Ryan G, Pandit A and Apatsidis D P 2006 Fabrication methods of porous metals for use in orthopaedic applications *Biomaterials* **27** 2651–70
[6] Hollander D A, Wirtz T, Von Walter M, Linker R, Schultheis A and Paar O 2003 Development of individual three-dimensional bone substitutes using 'selective laser melting' *Eur. J. Trauma* **29** 228–34
[7] Bhargav A, Sanjairaj V, Rosa V, Feng L W and Yh J F 2017 Applications of additive manufacturing in dentistry: a review *J. Biomed. Mater. Res.* B **106B** 2058–64
[8] Strietzel R 2010 Selective laser melting in dentistry *Informatics in Oral Medicine: Advanced Techniques in Clinical and Diagnostic Techniques* (Hershey, PA: ICI Global) pp 111–25
[9] Vandenbroucke B and Kruth J P 2008 Direct digital manufacturing of complex dental prostheses *Bio-Materials and Prototyping Applications in Medicine* (Boston, MA: Springer) pp 109–24
[10] Bibb R, Eggbeer D and Williams R 2006 Rapid manufacture of removable partial denture frameworks *Rapid Prototyping J.* **12** 95–9
[11] Shi J, Zhu L, Li L, Li Z, Yang J and Wang X 2018 A TPMS-based method for modeling porous scaffolds for bionic bone tissue engineering *Sci. Rep.* **8** 7395
[12] Cao X F, Song P J, Qiao Y J and Zhen P 2015 3D printing of bone tissue engineering scaffolds *Chin. J. Tissue Eng. Res.* **19** 4076–80
[13] Yoo D 2012 New paradigms in internal architecture design and freeform fabrication of tissue engineering porous scaffolds *Med. Eng. Phys.* **34** 762–76
[14] Melchels F P, Bertoldi K, Gabbrielli R, Velders A H, Feijen J and Grijpma D W 2010 Mathematically defined tissue engineering scaffold architectures prepared by stereolithography *Biomaterials* **31** 6909–16
[15] Leong K F, Chua C K, Sudarmadji N and Yeong W Y 2008 Engineering functionally graded tissue engineering scaffolds *J. Mech. Behav. Biomed. Mater.* **1** 140–52
[16] Leong K F, Cheah C M and Chua C K 2003 Solid freeform fabrication of three-dimensional scaffolds for engineering replacement tissues and organs *Biomaterials* **24** 2363–78
[17] Zein I, Hutmacher D W, Tan K C and Teoh S H 2002 Fused deposition modeling of novel scaffold architectures for tissue engineering applications *Biomaterials* **23** 1169–85
[18] Larsen R D, Svensson G K and Bjärngard B E 1975 The use of wedge filters to improve dose distribution with the partial rotation technique *Radiology* **117** 441–5

[19] Khaledy N, Arbabi A and Sardari D 2011 The effects of cutouts on output, mean energy and percentage depth dose of 12 and 14 MeV electrons *J. Med. Phys.* **36** 213–9

[20] Hsu S-H, Roberson P L, Chen Y, Marsh R B, Pierce L J and Moran J M 2008 Assessment of skin dose for breast chest wall radiotherapy as a function of bolus material *Phys. Med. Biol.* **53** 2593–606

[21] Evans P M, Hansen V N, Mayles W P M, Swindell W, Torr M and Yarnold J R 1995 Design of compensators for breast radiotherapy using electronic portal imaging *Radiother. Oncol.* **37** 43–54

[22] Verhey L J 1995 Immobilizing and positioning patients for radiotherapy *Semin. Radiat. Oncol.* **5** 100–14

[23] Allan E, Stanton A, Pye D, Collins C, Perry L, Filby M and Wilkinson J 1998 Fractionated high dose rate brachytherapy moulds—a precise treatment for carcinoma of the pinna *Radiother. Oncol.* **48** 277–81

[24] Molineu A, Followill D S, Balter P A, Hanson W F, Gillin M T, Huq M S, Eisbruch A and Ibbott G S 2005 Design and implementation of an anthropomorphic quality assurance phantom for intensity-modulated radiation therapy for the radiation therapy oncology group *Int. J. Radiat. Oncol. Biol. Phys.* **63** 577–83

[25] Shrimpton P C, Wall B F and Fisher E S 1981 The tissue-equivalence of the Alderson Rando anthropomorphic phantom for x-rays of diagnostic qualities *Phys. Med. Biol.* **26** 133–9

[26] Yaffe M J 1987 Anthropomorphic phantoms *US Patent Specification* 4638502

[27] Chan R, Manzke R, Stanton D A and Shechter G 2011 Anatomically and functionally accurate soft tissue phantoms and method for generating same *US Patent Application* 12/520326

[28] Khan F M and Gerbi B J 2012 *Treatment Planning in Radiation Oncology* (Philadelphia, PA: Kluwer)

[29] Thwaites D, Scalliet P, Leer J W and Overgaard J 1995 Quality assurance in radiotherapy. European society for therapeutic radiology and oncology advisory report to the commission of the European union for the 'Europe against cancer programme *Radiother. Oncol.* **35** 61–73

[30] Ferreira I H, Dutreix A, Bridier A, Chavaudra J and Svensson H 2000 The ESTRO-QUALity assurance network (EQUAL) *Radiother. Oncol.* **55** 273–84

[31] Peters L J, O'Sullivan B, Giralt J, Fitzgerald T J, Trotti A, Bernier J, Bourhis J, Yuen K, Fisher R and Rischin D 2010 Critical impact of radiotherapy protocol compliance and quality in the treatment of advanced head and neck cancer: results from TROG 02.02 *J. Clin. Oncol.* **28** 2996–3001

[32] Schweikard A 1995 Treatment planning method and apparatus for radiosurgery and radiation therapy *US Patent Specification* 5438125

[33] Ju S G, Kim M K, Hong C-S, Kim J S, Han Y, Choi D H, Shin D and Lee S B 2014 New technique for developing a proton range compensator with use of a 3-dimensional printer *Int. J. Radiat. Oncol. • Biol. • Phys.* **88** 453–8

[34] Kim S-W, Shin H-J, Kay C S and Son S H 2014 A customized bolus produced using a 3-dimensional printer for radiotherapy *PLoS One* **9** e110746

[35] Arenas M, Sabater S, Sintas A, Arguis M, Hernandez V, Arquez M, Lopez I, Rovirosa A and Puig D 2017 Individualized 3D scanning and printing for non-melanoma skin cancer brachytherapy: a financial study for its integration into clinical workflow *J Contemp. Brachyther.* **9** 270–6

[36] Ehler E D, Barney B M, Higgins P D and Dusenbery K E 2014 Patient specific 3D printed phantom for IMRT quality assurance *Phys. Med. Biol.* **59** 5763–73

[37] Meyer T, Quirk S, D'Souza M, Spencer D and Roumeliotis M 2018 A framework for clinical commissioning of 3D-printed patient support or immobilization devices in photon radiotherapy *J. Appl. Clin. Med. Phys.* **19** 499–505

[38] Harris B D, Nilsson S and Poole C M 2015 A feasibility study for using ABS plastic and a low-cost 3D printer for patient-specific brachytherapy mould design *Australas. Phys. Eng. Sci. Med.* **38** 399–412

[39] Butson M J, Cheung T, Yu P and Metcalfe P 2000 Effects on skin dose from unwanted air gaps under bolus in photon beam radiotherapy *Radiat. Meas.* **32** 201–4

[40] Robar J and Su S 2019 System and method for manufacturing bolus for radiotherapy using a three-dimensional printer *US Patent Specification* 10350435

[41] Canters R A, Lips I M, Wendling M, Kusters M, van Zeeland M, Gerritsen R M, Poortmans P and Verhoef C G 2016 Clinical implementation of 3D printing in the construction of patient specific bolus for electron beam radiotherapy for non-melanoma skin cancer *Radiother. Oncol.* **121** 148–53

[42] Burleson S, Baker J, Hsia A T and Xu Z 2015 Use of 3D printers to create a patient-specific 3D bolus for external beam therapy *J. Appl. Clin. Med. Phys.* **16** 5247

[43] Ehler E, Sterling D, Dusenbery K and Lawrence J 2018 Workload implications for clinic workflow with implementation of three-dimensional printed customized bolus for radiation therapy: a pilot study *PLoS One* **13** e0204944

[44] Łukowiak M, Jezierska K, Boehlke M, Więcko M, Łukowiak A, Podraza W, Lewocki M, Masojć B and Falco M 2017 Utilization of a 3D printer to fabricate boluses used for electron therapy of skin lesions of the eye canthi *J. Appl. Clin. Med. Phys.* **18** 76–81

[45] Park S-Y, Choi C H, Park J M, Chun M, Han J H and Kim J-I 2016 A patient-specific polylactic acid bolus made by a 3D printer for breast cancer radiation therapy *PLoS One* **11** e0168063

[46] Su S, Moran K and Robar J L 2014 Design and production of 3D printed bolus for electron radiation therapy *J. Appl. Clin. Med. Phys.* **15** 4831–4831

[47] Ricotti R, Ciardo D, Pansini F, Bazani A, Comi S, Spoto R, Noris S, Cattani F, Baroni G and Orecchia R 2017 Dosimetric characterization of 3D printed bolus at different infill percentage for external photon beam radiotherapy *Phys. Med.* **39** 25–32

[48] Markovic A 2017 3D printed bolus with flexible materials: treatment planning accuracy and practical aspects *Int. J. Radiat. Oncol. Biol. Phys.* **99** E696

[49] Park J M, Son J, An H J, Kim J H, Wu H-G and Kim J-I 2019 Bio-compatible patient-specific elastic bolus for clinical implementation *Phys. Med. Biol.* **64** 105006

[50] 2019 PLA-Flex, S SOFT PLA-Flex *Filament2Print* (https://filament2print.com/gb/special-pla/660-soft-pla-flex.html) (Accessed: 27 August 2019)

[51] Constantinou C and Harrington J C 1989 Tissue compensators made of solid water or lead for megavoltage x-ray radiotherapy *Med. Dosim.* **14** 41–7

[52] Spicka J, Fleury K and Powers W 1988 Polyethylene-lead tissue compensators for megavoltage radiotherapy *Med. Dosim.* **13** 25–7

[53] Chang S X, Cullip T J, Deschesne K M, Miller E P and Rosenman J G 2004 Compensators: an alternative IMRT delivery technique *J. Appl. Clin. Med. Phys.* **5** 15–36

[54] Skinner L, Fahimian B P and Yu A S 2019 Tungsten filled 3D printed field shaping devices for electron beam radiation therapy *PLoS One* **14** e0217757

[55] Mohan R and Grosshans D 2017 Proton therapy—present and future *Adv. Drug Deliv. Rev.* **109** 26–44

[56] Lee M-Y, Han B, Jenkins C, Xing L and Suh T-S 2016 A depth-sensing technique on 3D-printed compensator for total body irradiation patient measurement and treatment planning *Med. Phys.* **43** 6137–44

[57] Park S-Y, Kim J.-I., Joo Y H, Lee J C and Park J M 2017 Total body irradiation with a compensator fabricated using a 3D optical scanner and a 3D printer *Phys. Med. Biol.* **62** 3735–56

[58] Avelino S R, Silva L F and Miosso C J 2012 Use of 3D-printers to create intensity-modulated radiotherapy compensator blocks *Conf. Proc. IEEE Eng. Med. Biol. Soc.* **2012** 5718–21

[59] Zou W *et al* 2015 Potential of 3D printing technologies for fabrication of electron bolus and proton compensators *J. Appl. Clin. Med. Phys.* **16** 4959

[60] CIRS Atom® Dosimetry Verification Phantoms—CIRS (https://cirsinc.com/products/radiation-therapy/atom-dosimetry-verification-phantoms/) (Accessed: 28 August 2019)

[61] CIRS Pediatric Anthropomorphic Training Phantoms—CIRS (https://cirsinc.com/products/x-ray-fluoro/pediatric-anthropomorphic-training-phantoms/) (Accessed: 1 June 2019)

[62] Radiology Support Devices 2019 The Alderson Radiation Therapy Phantom (http://rsdphantoms.com/radiation-therapy/the-alderson-radiation-therapy-phantom/) (Accessed: 28 August 2019)

[63] Universal Medical 2019 RSD Transparent PIXY Phantom (https://universalmedicalinc.com/rsd-transparent-pixy-phantom.html) (Accessed: 28 August 2019)

[64] Tino R, Yeo A, Leary M, Brandt M and Kron T 2019 A systematic review on 3D-printed imaging and dosimetry phantoms in radiation therapy *Technol. Cancer Res. Treatment* **18** 31514632

[65] Filippou V and Tsoumpas C 2018 Recent advances on the development of phantoms using 3D printing for imaging with CT, MRI, PET, SPECT, and ultrasound *Med. Phys.* **45** e740–60

[66] Hazelaar C, Van Eijnatten M, Dahele M, Wolff J, Forouzanfar T, Slotman B and Verbakel W F A R 2018 Using 3D printing techniques to create an anthropomorphic thorax phantom for medical imaging purposes *Med. Phys.* **45** 92–100

[67] Kamomae T *et al* 2017 Three-dimensional printer-generated patient-specific phantom for artificial in vivo dosimetry in radiotherapy quality assurance *Phys. Med.* **44** 205–11

[68] Alssabbagh M, Tajuddin A A, Abdulmanap M and Zainon R 2017 Evaluation of 3D printing materials for fabrication of a novel multi-functional 3D thyroid phantom for medical dosimetry and image quality *Radiat. Phys. Chem.* **135** 106–12

[69] Yea J W, Park J W, Kim S K, Kim D Y, Kim J G, Seo C Y, Jeong W H, Jeong M Y and Oh S A 2017 Feasibility of a 3D-printed anthropomorphic patient-specific head phantom for patient-specific quality assurance of intensity-modulated radiotherapy *PLoS One* **12** 2017

[70] Hernandez-Giron I, den Harder J M, Streekstra G J, Geleijns J and Veldkamp W J H 2019 Development of a 3D printed anthropomorphic lung phantom for image quality assessment in CT *Phys. Med.* **57** 47–57

[71] Mayer R, Liacouras P, Thomas A, Kang M, Lin L and Simone C B 2015 3D printer generated thorax phantom with mobile tumor for radiation dosimetry *Rev. Sci. Instrum.* **86** 074301

[72] Jahnke P, Schwarz S, Ziegert M, Schwarz F B, Hamm B and Scheel M 2019 Paper-based 3D printing of anthropomorphic CT phantoms: feasibility of two construction techniques *Eur. Radiol.* **29** 1384–90

[73] Jahnke P, Schwarz F B, Ziegert M, Almasi T, Abdelhadi O, Nunninger M, Hamm B and Scheel M 2018 A radiopaque 3D printed, anthropomorphic phantom for simulation of CT-guided procedures *Eur. Radiol.* **28** 4818–23

[74] Nowak L J and Pawlowska E 2019 Technical Note: an algorithm and software for conversion of radiotherapy contour-sequence data to ready-to-print 3D structures *Med. Phys.* **46** 1829–32

[75] Leary M, Kron T, Keller C, Franich R, Lonski P, Subic A and Brandt M 2015 Additive manufacture of custom radiation dosimetry phantoms: an automated method compatible with commercial polymer 3D printers *Mater. Des.* **86** 487–99

[76] Leary M, Tino R, Keller C, Franich R, Yeo A, Lonski P, Kyriakou E, Kron T and Brandt M 2019 Additive manufacture of lung equivalent anthropomorphic phantoms: a method to control hounsfield number utilizing partial volume effect *J. Eng. Sci. Med. Diagnos. Ther.* **3** 011001

[77] Tino R, Leary M, Yeo A, Brandt M and Kron T 2019 Gyroid structures for 3D-printed heterogeneous radiotherapy phantoms *Phys. Med. Biol.* **64** 21NT05

[78] Okkalidis N 2018 A novel 3D printing method for accurate anatomy replication in patient-specific phantoms *Med. Phys.* **45** 4600–6

[79] Irnstorfer N, Unger E, Hojreh A and Homolka P 2019 An anthropomorphic phantom representing a prematurely born neonate for digital x-ray imaging using 3D printing: proof of concept and comparison of image quality from different systems *Sci. Rep.* **9** 14357

[80] Yoon K, Jeong C, Kim S-W, Cho B, Kwak J, Kim S S, Song S Y, Choi E K, Ahn S and Lee S-W 2018 Dosimetric evaluation of respiratory gated volumetric modulated arc therapy for lung stereotactic body radiation therapy using 3D printing technology *PLoS One* **13** e0208685

[81] Jakobsen A, Iversen P, Gadeberg C, Hansen J L and Hjelm-Hansen M 1987 A new system for patient fixation in radiotherapy *Radiother. Oncol.* **8** 145–51

[82] Dickens C 1981 Personalized fixation using a vacuum consolidation technique *Br. J. Radiol.* **54** 257–8

[83] Landberg T, Svahn-Tapper G and Bengtsson C-G 1977 Whole-body-casts for patient immobilization in mantle treatment, treatment of the inverted-Y and moving strip *Int. J. Radiat. Oncol. Biol. Phys.* **2** 809–13

[84] Bentel G C 1990 Positioning and immobilization device for patients receiving radiation therapy for carcinoma of the breast *Med. Dosim.* **15** 3–6

[85] Bentel G 1991 Positioning and immobilization of patients undergoing radiation therapy for Hodgkin's disease *Med. Dosim.* **16** 111–7

[86] Buscher M 1990 A modification of the HS3 thoracic Alpha Cradle for breast/chestwall patients *Med. Dosim.* **15** 19–20

[87] Frank L E, Rowley L A, Shanahan T G and Mehta M P 1990 Technical aspects in the use of 'belly boards' for small bowel minimization *Med. Dosim.* **15** 13–6

[88] Goldschmidt E J Jr and Holst R J 1990 Medulloblastoma immobilization and treatment considerations *Med. Dosim.* **15** 7–11

[89] Hook S and Pardy J 1990 Alpha cradles in breast cancer treatment: easy immobilization for the potentially difficult breast set up *Med. Dosim.* **15** 21–4

[90] Makino N, Kaneka M, Tanaka Y, Takai M, Fuwa N, Kitazawa S and Gotoh S 1984 Clinical applications of patient's positioning and immobilization using the rigid urethane foam *Rinsho. Hoshasen. Clin. Radiogr.* **29** 1135–8

[91] Makino N 1984 Improvement of the immobilization method in combination with a rigid urethane foam supporter and a thermoplastic cast *Nihon Igaku Hoshasen Gakkai zasshi. Nippon Radiol.* **44** 732

[92] Makino N 1984 Development of the head and neck immobilization device, using rigid polyurethane foam *Nihon Igaku Hoshasen Gakkai zasshi. Nippon Radiol.* **44** 714–26

[93] Gerber R, Marks J and Purdy J 1982 The use of thermal plastics for immobilization *Int. J. Radiat. Oncol. Biol. Phys.* **8** 1460–2

[94] Goldson A L, Young J Jr, Espinoza M C and Henschke U K 1978 Simple but sophisticated immobilization casts *Int. J. Radiat. Oncol. Biol. Phys.* **4** 1105–6

[95] Tsujii H, Mizoe J.-E., Arimoto T, Kamada T, Shirato H and Irie G 1984 Treatment planning with head and neck immobilization shell *Nippon Igaku Hoshasen Gakkai Zasshi* **44** 1391–5

[96] Verhey L J, Goitein M, McNulty P, Munzenrider J E and Suit H D 1982 Precise positioning of patients for radiation therapy *Int. J. Radiat. Oncol. Biol. Phys.* **8** 289–94

[97] Inoue T, Chatani M, Teshima T, Hata K, Izawa K and Sasaki J 1985 Immobilization and reproducibility in radiotherapy for cancer of the larynx and pharynx using simplified shell and bite-block *Strahlentherapie* **161** 642–5

[98] Wong J W, Binns W R, Cheng A Y, Geer L Y, Epstein J W, Klarmann J and Purdy J A 1990 On-line radiotherapy imaging with an array of fiber-optic image reducers *Int. J. Radiat. Oncol. Biol. Phys.* **18** 1477–84

[99] Dimitriadis A, Kirkby K J, Nisbet A and Clark C H 2016 Current status of cranial stereotactic radiosurgery in the UK *Br. J. Radiol.* **89** 20150452

[100] Stiegelis H E, Ranchor A V and Sanderman R 2004 Psychological functioning in cancer patients treated with radiotherapy *Patient Educ. Counsel.* **52** 131–41

[101] Sharp L, Lewin F, Johansson H, Payne D, Gerhardsson A and Rutqvist L E 2005 Randomized trial on two types of thermoplastic masks for patient immobilization during radiation therapy for head-and-neck cancer *Int. J. Radiat. Oncol. Biol. Phys.* **61** 250–6

[102] Oultram S, Findlay N, Clover K, Cross L, Ponman L and Adams C 2012 A comparison between patient self-report and radiation therapists' ability to identify anxiety and distress in head and neck cancer patients requiring immobilization for radiation therapy *J. Radiother. Pract.* **11** 74–82

[103] Goldsworthy S D, Tuke K and Latour J M 2016 A focus group consultation round exploring patient experiences of comfort during radiotherapy for head and neck cancer *J. Radiother. Pract.* **15** 143–9

[104] Haefner M F *et al* 2018 3D-Printed masks as a new approach for immobilization in radiotherapy—a study of positioning accuracy *Oncotarget* **9** 6490–8

[105] Laycock S D, Hulse M, Scrase C D, Tam M D, Isherwood S, Mortimore D B, Emmens D, Patman J, Short S C and Bell G D 2015 Towards the production of radiotherapy treatment shells on 3D printers using data derived from DICOM CT and MRI: preclinical feasibility studies *J. Radiother. Pract.* **14** 92–8

[106] Fisher M, Applegate C, Ryalat M, Laycock S, Hulse M, Emmens D and Bell D 2014 Evaluation of 3D printed immobilisation shells for head and neck IMRT *Open J. Radiol.* **4** 322–8

[107] Sousa E, Vieira L, Costa D, Costa D C, Parafita R and Loja A 2017 Comparison between 3D laser scanning and computed tomography on the modelling of head surface *3rd Int. Conf. Numerical and Symbolic Computation (SYMCOMP)* pp 119–28

[108] Loja M A R, Craveiro D S, Vieira L, Sousa E, Rodrigues J A and Portal R J F 2019 Radiotherapy-customized head immobilization masks: from modeling and analysis to 3D printing *Nucl. Sci. Tech.* **30** 142

[109] Michiels S *et al* 2016 Towards 3D printed multifunctional immobilization for proton therapy: initial materials characterization *Med. Phys.* **43** 5392–402

[110] Ostyn M, Wang S, Kim Y-S, Kim S and Yeo W-H 2019 Radiotherapy-compatible robotic system for multi-landmark positioning in head and neck cancer treatments *Sci. Rep.* **9** 1–9

[111] Cardenas M, Perks J and Benedict S 2019 A novel 3D-printed patient positioning platform to accommodate curved couch of MR scanner optimizes precision treatment planning workflow for abdominal radiotherapy *Int. J. Radiat. Oncol. Biol. Phys.* **105** S200–1

[112] Kitamori H, Sumida I, Tsujimoto T, Shimamoto H, Murakami S and Ohki M 2019 Evaluation of mouthpiece fixation devices for head and neck radiotherapy patients fabricated in PolyJet photopolymer by a 3D printer *Phys. Med.* **58** 90–8

[113] Burns L, Young S, Beaudry J, Gill B, Coope R and Duzenli C 2019 Rapid prototyping, design and early testing of a novel device for supine positioning of large volume or pendulous breasts in radiotherapy *World Congress on Medical Physics and Biomedical Engineering* (Singapore: Springer) pp 429–35

[114] Guinot J L, Rembielak A, Perez-Calatayud J, Rodríguez-Villalba S, Skowronek J, Tagliaferri L, Guix B, Gonzalez-Perez V, Valentini V and Kovacs G 2018 GEC-ESTRO ACROP recommendations in skin brachytherapy *Radiother. Oncol.* **126** 377–85

[115] Ouhib Z, Kasper M, Calatayud J P, Rodriguez S, Bhatnagar A, Pai S and Strasswimmer J 2015 Aspects of dosimetry and clinical practice of skin brachytherapy: the American Brachytherapy Society working group report *Brachytherapy* **14** 840–58

[116] Joslin C, Liversage W and Ramsey N 1969 High dose-rate treatment moulds by afterloading techniques *Br. J. Radiol.* **42** 108–12

[117] Sabbas A M, Kulidzhanov F G, Presser J, Hayes M K and Nori D 2004 HDR brachytherapy with surface applicators: technical considerations and dosimetry *Technol. Cancer Res. Treatment* **3** 259–67

[118] Laan R C, Nout R A, Dankelman J and van de Berg N J 2019 MRI-driven design of customised 3D printed gynaecological brachytherapy applicators with curved needle channels *3D Printing in Medicine* **5** 8

[119] Oare C, Wilke C, Ehler E, Mathew D, Sterling D and Ferreira C 2019 Dose calibration of Gafchromic EBT3 film for Ir-192 brachytherapy source using 3D-printed PLA and ABS plastics *3D Printi. Med.* **5** 3

[120] Baltz G C, Chi P-C M, Wong P-F, Wang C, Craft D F, Kry S F, Lin S S H, Garden A S, Smith S A and Howell R M 2019 Development and validation of a 3D-printed bolus cap for total scalp irradiation *J. Appl. Clin. Med. Phys.* **20** 89–96

[121] Kong Y, Yan T, Sun Y, Qian J, Zhou G, Cai S and Tian Y 2019 A dosimetric study on the use of 3D-printed customized boluses in photon therapy: a hydrogel and silica gel study *J. Appl. Clin. Med. Phys.* **20** 348–55

[122] Sasaki D K, McGeachy P, Aviles J E A, McCurdy B, Koul R and Dubey A 2019 A modern mold room: meshing 3D surface scanning, digital design, and 3D printing with bolus fabrication *J. Appl. Clin. Med. Phys.* **20** 78–85

[123] An H J, Kim M S, Kim J, Son J, Choi C H, Park J M and Kim J-I 2019 Geometric evaluation of patient-specific 3D bolus from 3D printed mold and casting method for radiation therapy *Prog. Med. Phys.* **30** 32–8

[124] Bustillo J P, Tumlos R and Remoto R Z 2019 Intensity modulated radiotherapy (IMRT) phantom fabrication using fused deposition modeling (FDM) 3D printing technique *World Congress on Medical Physics and Biomedical Engineering* (Singapore: Springer) pp 509–15

[125] Kadoya N, Abe K, Nemoto H, Sato K, Ieko Y, Ito K, Dobashi S, Takeda K and Jingu K 2019 Evaluation of a 3D-printed heterogeneous anthropomorphic head and neck phantom for patient-specific quality assurance in intensity-modulated radiation therapy *Radiol. Phys. Technol.* **12** 351–6

[126] Zhang F, Zhang H, Zhao H, He Z, Shi L, He Y, Ju N, Rong Y and Qiu J 2019 Design and fabrication of a personalized anthropomorphic phantom using 3D printing and tissue equivalent materials *Quant. Imaging Med. Surg.* **9** 94
[127] Niebuhr N I, Johnen W, Echner G, Runz A, Bach M, Stoll M, Giske K, Greilich S and Pfaffenberger A 2019 The ADAM-pelvis phantom-an anthropomorphic, deformable and multimodal phantom for MRgRT *Phys. Med. Biol.* **64** 04NT05
[128] Makris D N, Pappas E P, Zoros E, Papanikolaou N, Saenz D L, Kalaitzakis G, Zourari K, Efstathopoulos E, Maris T G and Pappas E 2019 Characterization of a novel 3D printed patient specific phantom for quality assurance in cranial stereotactic radiosurgery applications *Phys. Med. Biol.* **64** 105009
[129] Price E, Robinson A P, Cullen D M, Tipping J, Calvert N, Hamilton D, Oldfield C, Page E, Pietras B and Smith A 2019 Improving molecular radiotherapy dosimetry using anthropomorphic calibration *Phys. Med.* **58** 40–6
[130] He Y *et al* 2019 3D-printed breast phantom for multi-purpose and multi-modality imaging *Quant. Imaging Med. Surg.* **9** 63–74
[131] Wood S, Martins T and Ibrahim T S 2019 How to design and construct a 3D-printed human head phantom *J. 3D Print. Med.* **3** 119–25
[132] Grehn M, Stille M, Ziemann C, Cremers F, Rades D and Buzug T M 2019 A new phantom for individual verification of the dose distribution in precision radiotherapy for head-and-neck cancer *Anticancer Res.* **39** 6931–8
[133] Lancellotta V *et al* 2019 Individual 3-dimensional printed mold for treating hard palate carcinoma with brachytherapy: a clinical report *J. Prosthetic Dentistry* **121** 690–3
[134] Casey S, Bahl G and Awotwi-Pratt J B 2019 High dose rate 192-Ir-brachytherapy for basal cell carcinoma of the skin using a 3D printed surface mold *Cureus* **11** e4913–4913
[135] Bassi S, Langan B and Malone C 2019 Dosimetry assessment of patient-specific 3D printable materials for HDR surface brachytherapy *Phys. Med.* **67** 166–75
[136] Park S-Y, Kang S, Park J M, An H J, Oh D H and Kim J-I 2019 Development and dosimetric assessment of a patient-specific elastic skin applicator for high-dose-rate brachytherapy *Brachytherapy* **18** 224–32
[137] Chmura J, Erdman A, Ehler E, Lawrence J, Wilke C T, Rogers B and Ferreira C 2019 Novel design and development of a 3D-printed conformal superficial brachytherapy device for the treatment of non-melanoma skin cancer and keloids *3D Print. Med.* **5** 10
[138] D'Alimonte L, Ravi A, Helou J, Morrison D, Mendez L C, Easton H and Morton G 2019 Optimized penile surface mold brachytherapy using latest stereolithography techniques: a single-institution experience *Brachytherapy* **18** 348–52
[139] Imber B S, Wolden S L, Stambuk H E, Matros E, Wexler L H, Drew A S, Rosen E B, Ganly I, Cohen G A N and Damato A L 2019 Novel intraoperative radiotherapy utilizing prefabricated custom three-dimensionally printed high-dose-rate applicators *Brachytherapy* **18** 277–84
[140] Zhao Z, Tang X, Mao Z and Zhao H 2019 The design of an individualized cylindrical vaginal applicator with oblique guide holes using 3D modeling and printing technologies *J. Contemp. Brachyther.* **11** 479–87
[141] Taggar A, Barnes E, Martell K, Ahmed B, Paudel M and Ravi A 2019 3D printed individually customized high-dose-rate brachytherapy applicator for treatment of chronic digital psoriasis *Brachytherapy* **18** S22
[142] Hodgdon T *et al* 2018 Logistics of three-dimensional printing: primer for radiologists *Acad. Radiol.* **25** 40–51
[143] Ballard D H *et al* 2018 Clinical applications of 3D printing: primer for radiologists *Acad. Radiol.* **25** 52–65
[144] Frazer J 2002 Creative design and the generative evolutionary paradigm *Creative Evolutionary Systems* (Amsterdam: Elsevier) pp 253–74
[145] Leary M (ed) 2019 *Design for Additive Manufacturing* 1st edn (Sydney: Elsevier) p 358
[146] Au A K, Lee W and Folch A 2014 Mail-order microfluidics: evaluation of stereolithography for the production of microfluidic devices *Lab. Chip.* **14** 1294–301
[147] Wood S, Krishnamurthy N, Santini T, Raval S, Farhat N, Holmes J A and Ibrahim T S 2017 Design and fabrication of a realistic anthropomorphic heterogeneous head phantom for MR purposes *PLoS One* **12** e0183168
[148] Brunelle M, Ferralli I, Whitsitt R and Medicus K 2017 Current use and potential of additive manufacturing for optical applications *Proc. SPIE* **10448** 104480P
[149] Van der Veen A C, Coenders J, Veer F, Nijsse R, Houtman R and Schonwalder J 2015 The structural feasibility of 3D-printing houses using printable polymers *Proc. Int. Association for Shell and Spatial Structures (IASS) Symp. Future Visions (Amsterdam, The Netherlands, 17–20 August 2015)*
[150] Skylar-Scott M A, Mueller J, Visser C W and Lewis J A 2019 Voxelated soft matter via multimaterial multinozzle 3D printing *Nature* **575** 330–5
[151] Soultanidis G *et al* 2019 Development of an anatomically correct mouse phantom for dosimetry measurement in small animal radiotherapy research *Phys. Med. Biol.* **64** 12NT02
[152] Bader C, Kolb D, Weaver J C, Sharma S, Hosny A, Costa J and Oxman N 2018 Making data matter: voxel printing for the digital fabrication of data across scales and domains *Sci. Adv.* **4** eaas8652
[153] Hosny A *et al* 2018 From improved diagnostics to presurgical planning: high-resolution functionally graded multimaterial 3D printing of biomedical tomographic data sets *3D Print. Additive Manuf.* **5** 103–13
[154] Stratasys 2019 J750^{TM} Digital Anatomy^{TM} 3D Printer (https://stratasys.com/3d-printers/j750-digital-anatomy) (Accessed: 8 September 2019)
[155] Keall P J, Mageras G S, Balter J M, Emery R S, Forster K M, Jiang S B, Kapatoes J M, Low D A, Murphy M J and Murray B R 2006 The management of respiratory motion in radiation oncology report of AAPM Task Group 76 a *Med. Phys.* **33** 3874–900
[156] Brock K K, Mutic S, McNutt T R, Li H and Kessler M L 2017 Use of image registration and fusion algorithms and techniques in radiotherapy: report of the AAPM radiation therapy committee task group No. 132 *Med. Phys.* **44** e43–76
[157] Aerts H J *et al* 2014 Decoding tumour phenotype by noninvasive imaging using a quantitative radiomics approach *Nat. Commun.* **5** 4006
[158] Kumar V *et al* 2012 Radiomics: the process and the challenges *Magn. Reson. Imaging* **30** 1234–48
[159] Sanduleanu S, Woodruff H C, de Jong E E C, van Timmeren J E, Jochems A, Dubois L and Lambin P 2018 Tracking tumor biology with radiomics: a systematic review utilizing a radiomics quality score *Radiother. Oncol.* **127** 349–60
[160] van Timmeren J E, Leijenaar R T H, van Elmpt W, Reymen B, Oberije C, Monshouwer R, Bussink J, Brink C, Hansen O and Lambin P 2017 Survival prediction of non-small cell lung cancer patients using radiomics analyses of cone-beam CT images *Radiother. Oncol.* **123** 363–9
[161] Larue R *et al* 2018 Pre-treatment CT radiomics to predict 3-year overall survival following chemoradiotherapy of esophageal cancer *Acta Oncol.* **57** 1475–81
[162] Traverso A, Wee L, Dekker A and Gillies R 2018 Repeatability and reproducibility of radiomic features: a systematic review *Int. J. Radiat. Oncol. Biol. Phys.* **102** 1143–58

[163] Plautz T E, Zheng C, Noid G and Li X A 2019 Time stability of delta-radiomics features and the impact on patient analysis in longitudinal CT images *Med. Phys.* **46** 1663–76
[164] NIH 3D Print Exchange 2019 A collection of biomedical 3D printable files and 3D printing resources supported by the National Institutes of Health (NIH) (https://3dprint.nih.gov/) (Accessed: 8 September 2019)
[165] RSNA 2019 RSNA and ACR to Collaborate on Landmark Medical 3D Printing Registry (https://rsna.org/en/news/2019/August/3D-Printing-Registry) (Accessed: 5 October 2019)
[166] Ehler E, Craft D and Rong Y 2018 3D printing technology will eventually eliminate the need of purchasing commercial phantoms for clinical medical physics QA procedures *J. Appl. Clin. Med. Phys.* **19** 8–12
[167] IEEE 2011 IEEE Guide—Adoption of the Project Management Institute (PMI®) Standard 4th edn A Guide to the Project Management Body of Knowledge (PMBOK® Guide) pp 39–47
[168] Sigaux N, Pourchet L, Breton P, Brosset S, Louvrier A and Marquette C A 2019 3D Bioprinting:principles, fantasies and prospects *J. Stomatol., Oral Maxillofacial Surg.* **120** 128–32